New Interactive Methods for Tubular Structure Segmentation on Medical Images

F. Benmansour[1], L.D. Cohen[1], E.E. Dávila Serrano[2], P.C. Douek[2], M. Orkisz[2], M.A. Zuluaga[2]

March 24, 2009

[1] CEREMADE, CNRS UMR7534, Université Paris Dauphine, Place du Maréchal de Lattre de Tassigny, 75775 Paris Cedex 16 - France
e-mail: benmansour, cohen@ceremade.dauphine.fr
[2] Université de Lyon; Université Lyon 1; INSA-Lyon; CNRS UMR5220; Inserm U630; CREATIS-LRMN; Villeurbanne, France
e-mail: davila, douek, orkisz, zuluaga@creatis.univ-lyon1.fr

Abstract

In this paper we present two interactive methods for tubular structure fast extraction. The main application and motivation for this work is vessel tracking in 2D and 3D medical images. The basic tools are minimal paths solved using the fast marching algorithm. This allows interactive tools for the physician by clicking on a small number of points in order to obtain a minimal path between two points or a set of paths in the case of a tree structure. Visualization tools are very important in order to choose points and show paths and vessels in the case of 3D images. We show variants of the minimal path method that differ both on the model used (path on the image domain or centerline and surface by adding one dimension for the local radius around the centerline), the way the endpoints are chosen by the user (two points or automatic detection of key points from a single click) and the definition of the local metrics to minimize (based on gray level or also on the local orientation using a Riemannian metrics). The algorithms were made available for the physician by use of a new programming framework called CreaTools. This software suite was used to build a Graphical User Interface (GUI) and to connect the different processing methods. The GUI provides the necessary visualization and interaction for parameter tuning, source point definition and analysis of the outcome. We show results on various CT images.

1 Introduction

Coronary artery disease (CD) is the leading cause of death in the United States. In symptomatic patients, diagnosis of the presence and severity of coronary artery disease is critical for determining appropriate clinical management. Indirect evaluation of coronary stenosis, such as through stress testing, has limited diagnostic ability as compared with direct conventional coronary angiography. Conventional coronary angiography reveals the extent, location, and severity of coronary obstructive lesions, which are potent

predictors of outcome, and identifies high-risk patients who may benefit from revascularization. Thus, invasive coronary angiography, despite the associated risks, remains the standard for the diagnosis of obstructive coronary artery disease. Multidetector computed tomographic (MDCT) angiography has been proposed as a noninvasive test to determine the presence of CD. Although MDCT angiographic data acquisition is straightforward, effective visualization and communication of the complex multifocal manifestations of CD remain a major challenge. For accurate image interpretation, precise, fast and semiautomatic image processing tools are mandatory.

During the last two decades, the extraction of vascular objects (in 2D or 3D images) such as the blood vessels, coronary arteries, or other tube-like structures has attracted the attention of more and more researchers. Various methods such as vascular image enhancement methods [15, 17, 10, 6, 13], vessel-tracking [1, 19, 16] or others were proposed, see [4, 9] for wider surveys. Despite the existence of more or less interactive tools on clinical consoles, fast and accurate vessel segmentation remains a challenge, particularly when dealing with thin vascular tree structures such as the coronary arteries [14].

Some of the existing methods extract the vessel boundary directly, and then use thinning methods or a generalized cylindrical model (e.g. [5]) to find its center line. Other methods (e.g. [7]) first extract the center line and then extract its boundary as a stacking of cross-sectional contours. Deschamps and Cohen [3] proposed to use the minimal paths method to find the center line. The minimal path technique introduced by Cohen and Kimmel [2] captures the global minimum curve between two points given by the user. This leads to the global minimum of an active contour energy. Since then, the minimal paths method has been improved by many researchers, and adapted to anisotropic media as done by Jbabdi *et al.* for *tractography* [8]. Unfortunately, despite their numerous advantages, classical minimal path techniques exhibit some disadvantages. First, vessel boundary extraction can be very difficult, especially for coronary arteries. This is true even in 2D where the vessel boundary can be completely described by two curves. Second, the path given by the minimal path technique does not always yield the precise center line of the vessel. A readjustment is required to obtain a central trajectory. Third, the minimal paths technique provides only a trajectory and does not give information about the vessel boundary.

The methods we propose here are generic and can be used for extracting tubular structures in various applications, although we are motivated by the segmentation of coronary and pulmonary arteries. The first method builds on a variant of the minimal path approach. First, an initial point on the object is chosen by the user. Next, new key points are detected automatically using a front propagation approach. These points are automatically detected using a criterion based on the Euclidean length of minimal paths and are almost equi-distributed along the structure of interest. Two different stopping criteria are proposed. The first one needs more interaction by specifying an endpoint to reach. The second one is based on an approximation of the total length: the propagation and key point detection are stopped as soon as a maximal total path length given by the user is reached.

The second method we propose is based on a variant of the classical, purely spatial, minimal paths technique by incorporating an extra *non-spatial* dimension into the search space. This approach was first proposed by Li and Yezzi [12]. Each point of the 4D path (after adding the extra dimension for the 3D image) consists of three spatial coordinates plus a fourth coordinate which describes the vessel thickness at that corresponding 3D point. Thus each 4D point represents a sphere in 3D space, and the vessel is obtained by

taking the envelope of these spheres as we move along the 4D curve. The main drawback of the cited method is that only isotropic media were considered, which does not take into account the orientation of the vessels. Our first contribution for this method is to take into account the vessel orientation by defining a suited anisotropic metric that makes the propagation faster along the center lines and for the adequate radius. The second contribution is to build an anisotropic metric based on the *Optimally Oriented Flux* (OOF) descriptor. The OOF was first presented by Law and Chung in [11]. Its main advantage is that the disturbance introduced by the closely located nearby structures is avoided. But they did not exploit the orientations given by the OOF. We propose to do so by using the OOF's scalar functions as well as its orientation. This contributes to make the propagation faster along the vessel's center line and at exact associated scale, i.e.: the path location, orientation and scale (radius) have to be coherent with the local geometry of the image extracted by the OOF.

In section 2, we give some background on minimal paths method and Anisotropic Fast Marching. In section 3 the recursive key points detection method is presented and some results are shown on pulmonary arteries. In section 4 the tubular anisotropy method is presented as well as some results on coronary arteries. The CreaTools software suite, used to implement the algorithms within a Graphical User Interface (GUI) is presented in section 5. Finally, conclusions and perspectives follow in section 6.

2 Background on minimal paths method

A minimal path is a pathway minimizing the energy functional:

$$E(\gamma) = \int_{\gamma} \mathcal{P}\big(\gamma(s), \gamma'(s)\big)\mathrm{d}s, \tag{1}$$

where $\mathcal{P}(\gamma, \gamma') = \sqrt{\gamma'^T \mathcal{M}(\gamma)\gamma'}$ describes an infinitesimal distance along a pathway γ relative to a metric tensor $\mathcal{M}$ (symmetric definite positive). It was first introduced in the isotropic case [2], i.e. with $\mathcal{P}$ that does not depend on its second variable. $\mathcal{M}$ is defined from some features extraction in the image. A curve connecting $\mathbf{p}_1$ to $\mathbf{p}_2$ that globally minimizes the above energy (1) is a *minimal path* between $\mathbf{p}_1$ and $\mathbf{p}_2$, noted $\mathcal{C}_{\mathbf{p}_1,\mathbf{p}_2}$. The solution of this minimization problem is obtained through the computation of the *minimal action map* $\mathcal{U}_1 : \Omega \to \mathbb{R}^+$ associated to $\mathbf{p}_1$. The minimal action is the minimal energy integrated along a path between $\mathbf{p}_1$ and any point $\mathbf{x}$ of the domain Ω :

$$\forall\ \mathbf{x} \in \Omega,\ \mathcal{U}_1(\mathbf{x}) = \min_{\gamma \in \mathcal{A}_{\mathbf{p}_1,\mathbf{x}}} \left\{ \int_{\gamma} \mathcal{P}\big(\gamma(s), \gamma'(s)\big)\mathrm{d}s \right\}. \tag{2}$$

The values of $\mathcal{U}_1$ may be regarded as the arrival times of a front propagating from the source $\mathbf{p}_1$ with oriented velocity related to the metric tensor $\mathcal{M}^{-1}$. $\mathcal{U}_1$ satisfies the Eikonal equation

$$\|\nabla \mathcal{U}_1(\mathbf{x})\|_{\mathcal{M}^{-1}(\mathbf{x})} = 1 \text{ for } \ \mathbf{x} \in \Omega, \text{ and } \mathcal{U}_1(\mathbf{p}_1) = 0, \tag{3}$$

where $\|\mathbf{v}\|_M = \sqrt{\mathbf{v}^T M \mathbf{v}}$. The flow lines of $\mathcal{U}_1$ satisfy the Euler-Lagrange equation of functional (1). Thus, the minimal path $\mathcal{C}_{\mathbf{p}_1,\mathbf{p}_2}$ can be retrieved with a simple gradient descent on $\mathcal{U}_1$ from $\mathbf{p}_2$ to $\mathbf{p}_1$ (see Fig. 1). Proof of (3) can be found in [18, 8]. On figure 1, we show some examples of the minimal paths method on an isotropic case and an anisotropic one. On the first image of figure 1 the metric is isotropic and the potential

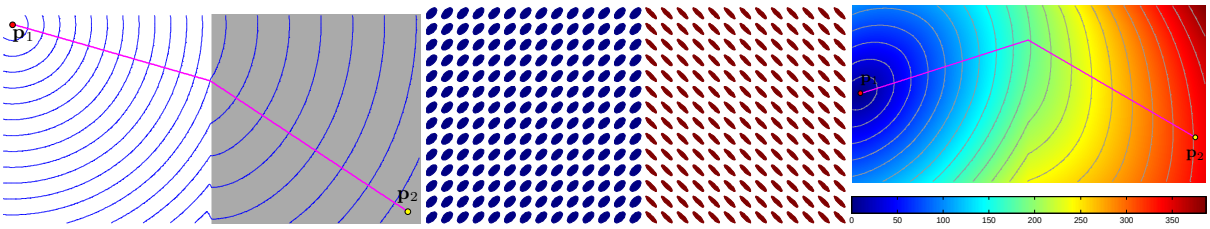

Figure 1: Minimal paths examples. **Left**: an isotropic case on the left image. **Middle**: anisotropic metric, constant on each half side of the image, displayed by equivalent ellipses, i.e. the axes-ratio of which is equal to the ratio of the eigenvalues. **Right**: minimal action map associated to the source point $\mathbf{p}_1$, with the minimal path $\mathcal{C}_{\mathbf{p}_1,\mathbf{p}_2}$ superimposed.

in the gray region is twice as low as the white one. Iso-level sets of the minimal action map associated to the source point $\mathbf{p}_1$ and the minimal path $\mathcal{C}_{\mathbf{p}_1,\mathbf{p}_2}$ are displayed. The second image represents a metric $\mathcal{M}$. We took two constant metrics in each half side of the image. On the last image, the minimal action map $\mathcal{U}_1$ associated to the metric $\mathcal{M}$ and to the source point $\mathbf{p}_1$ is shown. The minimal path $\mathcal{C}_{\mathbf{p}_1,\mathbf{p}_2}$ is found by a simple gradient descent. The anisotropic Eikonal equation is solved using the Fast Marching algorithm. Descriptions and details on the isotropic and anisotropic Fast Marching can be found in [2, 18, 8].

3 Recursive key points detection

The idea is to recursively detect new source points (called key points) along the object of interest starting from a single point (or more if desired). This is done by use of front propagation approach and the final domain visited by the front yields a segmentation of the object of interest. The key points are automatically detected using a criterion based on the Euclidean length of minimal paths and are almost equi-distributed along the curve. In [3] it was proposed to use the length of the minimal path in order to find the second extremity of a path. Here we iterate this idea many times in order to obtain intermediate points along the object. At each iteration, we consider the set of key points as source points. Since the front is expected to propagate faster on the features, the first point for which a given length λ is reached, is located in this area (of small values of the potential) and is a valuable choice as a key point. A good choice of λ enables the front to propagate further in the direction of the thin tubular structures without propagating in all directions and thus to reduce considerably the visited domain on the image.

We implemented several stopping criteria. The simplest one is the maximal number of key points to add. However, this criterion is not intuitive enough to tune and is very dependent on the desired object and on the Euclidean length parameter λ. Another stopping criterion is based on the *total path length*. This criterion makes use of prior medical knowledge of the typical length of the vessel of interest. Here we also assume that only one single point is provided by the user, i.e. $\mathbf{p}_1$, and the idea is to detect automatically the key points until a fixed total length of the minimal path is reached. The third criterion requires that the user provide a destination point, in addition to the source point. Then the algorithm can stop as soon as the destination is reached.

In high-contrast vessels, e.g. pulmonary arteries (fig. 2), the method can provide a good segmentation even when using potentials $\mathcal{P}$ directly based on image intensities.

However, despite the use of the contrast agent, the intensities of the arteries in CT images may be similar to other neighboring structures, e.g. the coronary arteries can hardly be separated from blood-filled heart cavities. Hence, vessel enhancement filters [17, 6] were evaluated to construct a potential map for coronary arteries segmentation. The best experimental results were obtained by use of a modified version of the Frangi's multiscale filter. This version only includes the elongation and cross-sectional circularity terms, while the Frobenius norm term was removed.

4 Tubular anisotropy

This method is also minimally interactive. First, the user has to specify if the desired vessels are darker or brighter than the background. Then the scale range $[r_{\min}, r_{\max}]$, which corresponds to the range of radii of the vessels one wants to extract, is given by the user. Finally, few points are required as source points or end points of the Fast Marching algorithm.

As presented in section 2, the Fast Marching algorithm is a front propagation algorithm. The propagating front is guided by the metric $\mathcal{M}$. Therefore, the result given by the anisotropic minimal paths method is very dependent on the metric, results inherit advantages and drawbacks of the constructed metric, thus we should be very careful with its construction. Since the OOF descriptor avoids the disturbance introduced by the closely located nearby structures and gives an estimate of the orientation of the vessels, we chose to combine the scalar functions and the orientations given by the OOF to construct the 4D metric $\mathcal{M}$. The constructed metric makes the propagation faster along the center line of the vessel and when the radius is equal to the thickness of the vessel and thus the minimal path follows the estimated orientation.

On figure 3, left anterior descending (LAD) coronary artery as well as right coronary artery (RCA) are segmented using the tubular anisotropy method. One can see that the obtained radii of the principal coronary branches are larger than those of the secondary ones. Thus, our approach is robust to scale changing and bifurcations. Nevertheless, our current implementation requires huge memory allocations due to the 4D and anisotropic aspects.

5 Implementation using CreaTools

Although the methods presented are semi-automatic, interactive user interface is required both for initialization (selection of 3D points, adjustment of parameter value involved in the stopping criterion) and for the visual inspection of the results. Such a GUI is to be very user-friendly, built-up with high-level widgets, so as to be available for physicians. Furthermore, the algorithm-refining phase requires additional *ad hoc* interactive tools for internal parameter tuning, volume-of-interest selection, etc. These usually very complex development issues were made much easier by use of the CreaTools software suite.

This suite (`http://www.creatis.insa-lyon.fr/creatools/`) includes software and development tools (libraries, utilities...) for medical image processing and visualization. The CreaTools are open-source and cross-platform (Windows, Linux, MacOSX). One of the main characteristics of the suite is that it manages within a single framework heterogeneous third party libraries (itk, vtk, wxWidgets, KWWidgets ...), as well as

custom components. Thus, various processing methods and interactive widgets from different libraries can be interconnected to form pipelines, and properly executed.

One of the most interesting components of the CreaTools is the Black Box Toolkit (`bbtk`). It is a complete framework for prototyping, testing and creating demonstrators of new medical-image or mesh processing methods. According to its name, `bbtk` is based on the *black box* concept, i.e. any C/C++ processing algorithm or interactive widget is wrapped into a generic symbolic interface usable both in C++ programming and via a very simple scripting language called `bbs`. Numerous useful black boxes are already available in standard packages, and new packages can easily be added via a plug-in mechanism. The framework includes a script interpreter called `bbi`. The scripts can be edited and tested within a graphical development environment called `bbStudio`, which also provides detailed help on the black boxes, packages and the scripting language. The help on the black boxes and packages exploits an auto-documentation mechanism. The use of `bbStudio` permits to design very quickly small applications including nevertheless high-level components: GUI, data readers/writers, image/mesh viewers, interactors, etc. Amongst them, let us quote:

- the `Gimmick!` widget that handles many image formats, including DICOM, and allows the user to preview the images and organize them into DICOM tree-structure (Patient / Study / Series / Images) that are stored in databases and thus can be retrieved very quickly; this black box is provided as part of the `bbtk` package `creaImageIO`;
- the `creaMaracasVisu` package that provides advanced 3D image visualization and interaction widgets particularly well suited for vascular applications.

6 Conclusions

In this paper we have proposed two different methods for 3D tubular structure extraction. Both are semi-automatic, i.e. user interaction is only required at the initialization stage involving the selection of one or several points and of the parameter value used in the stopping criterion. The first method is very fast and allows to obtain a coherent segmentation of tubular structures when the desired vessels are well contrasted in the image. If not, an enhancement pre-processing step is required. The second method is more precise and more adequate for challenging vessels segmentation like coronary arteries. It is however much more time-consuming. We are currently working on its new implementation, in order to both reduce the computational time and save on memory allocations. Both methods were made available for the physicians via an appropriate GUI. The applications were developed by use of a new software suite CreaTools. We obtain promising results on medical data. In the future, we will work on medical validation of the methods.

7 Acknowledgements

This work has been partly supported by ECOS-Nord project #C07M04 and by Région Rhône-Alpes project PP3/I3M. M.A. Zuluaga's PhD project is supported by a Colciencias grant.

References

[1] S.R. Aylward and E. Bullitt. Initialization, noise, singularities and scale in height ridge traversal for tubular object centerline extraction. *IEEE Trans Med Imaging*, 21(2):61–75, 2002.

[2] L.D. Cohen and R. Kimmel. Global minimum for active contour models: a minimal path approach. *Int J Comput Vision*, **24**:57–78, 1997.

[3] T. Deschamps and L.D. Cohen. Fast extraction of minimal paths in 3D images and applications to virtual endoscopy. *MedIA*, 5(4):281–299, December 2001.

[4] J.S. Duncan and N. Ayache. Medical image analysis: Progress over two decades and the challenges ahead. *IEEE Trans PAMI*, 22(1):85–106, January 2000.

[5] L. Flórez Valencia, J. Azencot, F. Vincent, M. Orkisz, and I.E. Magnin. Segmentation and Quantification of Blood Vessels in 3D Images using a Right Generalized Cylinder State Model. In *Proc. IEEE International Conference on Image Processing*, pages 2441–2444, Atlanta, GA, USA, October 2006.

[6] A.F. Frangi, W.J. Niessen, K.L. Vincken, and M.A. Viergever. Multiscale vessel enhancement filtering. In *MICCAI*, volume LNCS 1496, pages 130–137. Springer-Verlag, 1998.

[7] M. Hernández Hoyos, M. Orkisz, P.C. Douek, and I.E. Magnin. Assessment of carotid artery stenoses in 3D contrast-enhanced magnetic resonance angiography, based on improved generation of the centerline. *Mach Graphics & Vision*, 14(4):349–378, 2005.

[8] S. Jbabdi, P. Bellec, R. Toro, J. Daunizeau, M. Pélégrini-Issac, and H. Benali. Accurate anisotropic fast marching for diffusion-based geodesic tractography. *J Biomed Imaging*, 2008(1):1–12, 2008.

[9] C. Kirbas and F.K.H. Quek. A review of vessel extraction techniques and algorithms. *ACM Computing Surveys*, 36:81–121, 2004.

[10] K. Krissian. Flux-based anisotropic diffusion applied to enhancement of 3D angiogram. *IEEE Trans Med Imag*, 21(11):1440–1442, 2002.

[11] M.W.K. Law and A.C.S. Chung. Three dimensional curvilinear structure detection using optimally oriented flux. *ECCV*, **4**:368–382, 2008.

[12] H. Li and A. Yezzi. Vessels as 4D curves: Global minimal 4D paths to extract 3D tubular surfaces and centerlines. *IEEE Trans Med Imag*, 26(9):1213–1223, 2007.

[13] Q. Li, S. Sone, and K. Doi. Selective enhancement filters for nodules, vessels, and airway walls in two- and three-dimensional CT scans. *Med Phys*, 30(8):2040–2051, 2003.

[14] C.T. Metz, M. Schaap, T. van Walsum, A. van der Giessen, A. Weustink, N.R.A. Mollet, G.P. Krestin, and W. Niessen. 3D Segmentation in the Clinic: A Grand Challenge II - Coronary Artery Tracking. *Midas Journal*, http://hdl.handle.net/10380/1399, 2008.

[15] M. Orkisz, C. Bresson, I.E. Magnin, O. Champin, and P.C. Douek. Improved vessel visualization in MR angiography by nonlinear anisotropic filtering. *Magn Reson Med*, 37(6):914–919, 1997.

[16] M. Orkisz, L. Flórez Valencia, and M. Hernández Hoyos. Models, algorithms and applications in vascular image segmentation. *Mach Graphics & Vision*, 17(1/2):5–33, 2008.

[17] Y. Sato, S. Nakajima, N. Shiraga, H. Atsumi1, S. Yoshida, T. Koller, G. Gerig, and R. Kikinis. Three-dimensional multi-scale line filter for segmentation and visualization of curvilinear structures in medical images. *MedIA*, 2(2):143–168, 1998.

[18] J.A. Sethian and A. Vladimirsky. Fast methods for the Eikonal and related Hamilton-Jacobi equations on unstructured meshes. *Proc Nat Acad Sc USA*, 97(11):5699–5703, May 2000.

[19] H. Shikata, E. Hoffman, and M. Sonka. Automated segmentation of pulmonary vascular tree from 3D CT images. In *Proc. SPIE Int. Symp. Medical Imaging*, volume 5369, pages 107–116, San Diego, CA, USA, 2004.

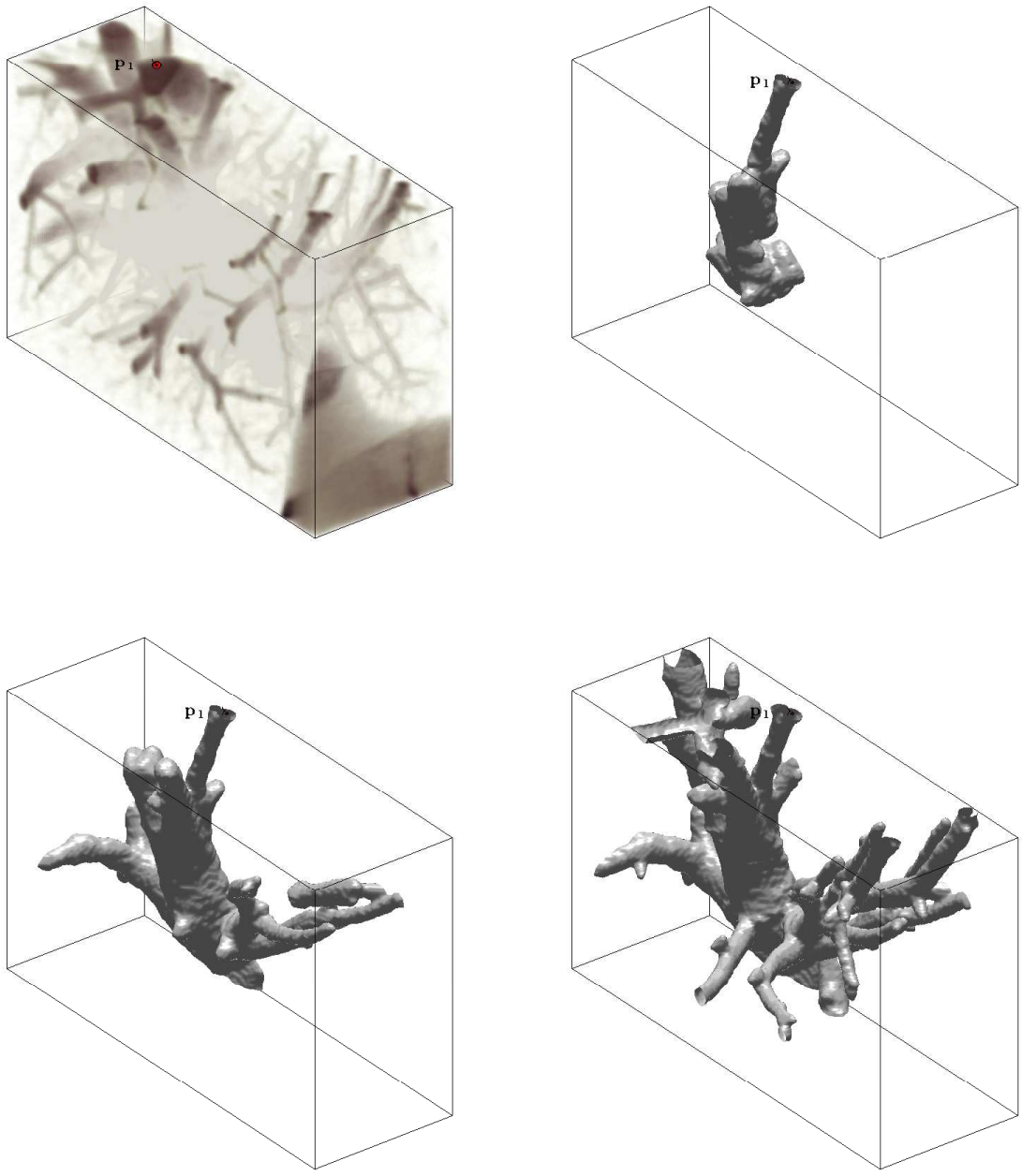

Figure 2: Original 3D image (transparent visualization of a part of a pulmonary arterial tree) and different steps of the Recursive Keypoints Detection approach from a single source point $\mathbf{p}_1$: segmentation obtained using marching cubes on the visited domain.

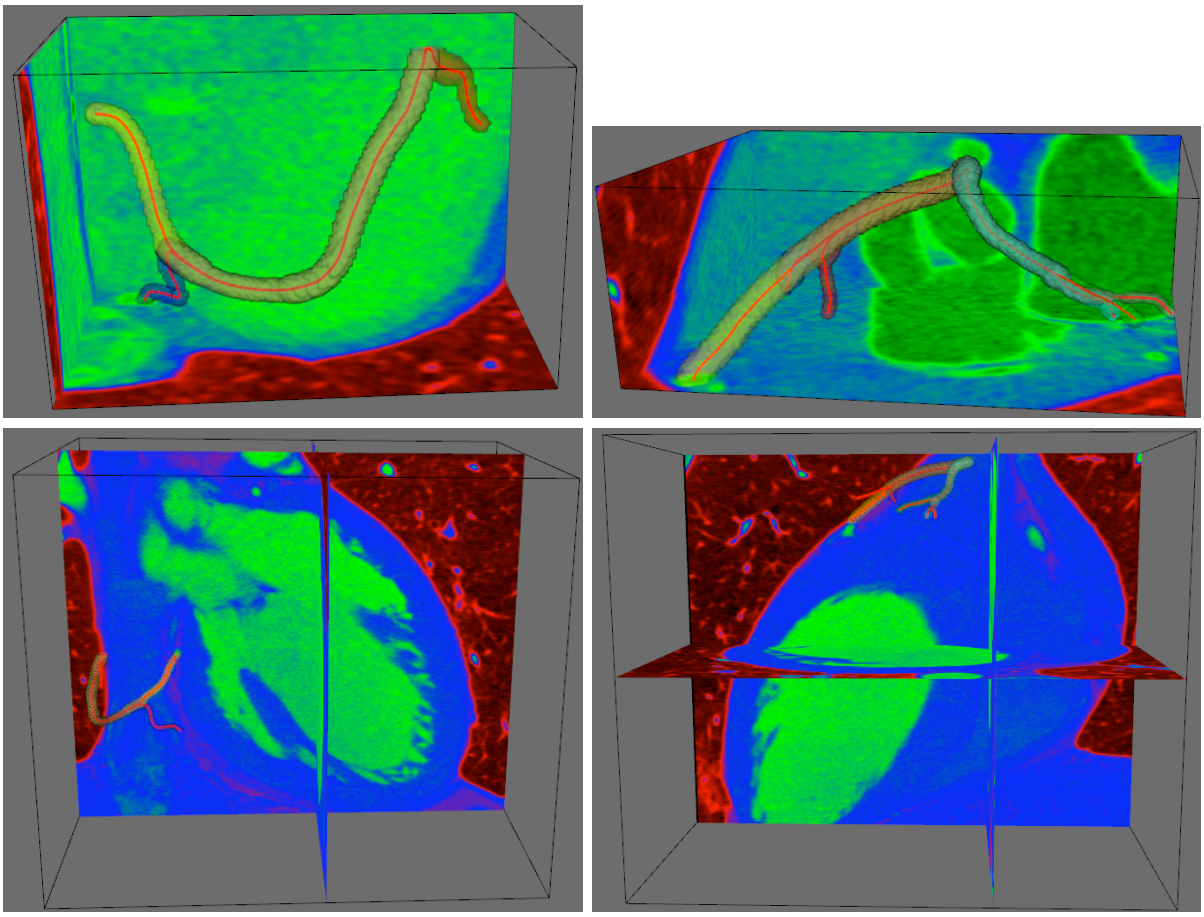

Figure 3: Coronary artery segmentation using the Tubular Anisotropy Method. **Left**: LAD and its branches. **Right**: RCA and its branches. The upper raw represents the selected sub-volumes of interest, while the lower row shows the segmented arteries within the whole image. Only few source points were required (the extremities of the paths). The method provides the center line as well as vessels boundaries.